Thesis for the Degree of Licentiate of Engineering

Evaluation of Radio-over-Fiber Technologies for Distributed MIMO

Frida Olofsson

Microwave Electronics Laboratory
Department of Microtechnology and Nanoscience – MC2
Chalmers University of Technology
Gothenburg, Sweden 2024

Evaluation of Radio-over-Fiber Technologies for Distributed MIMO

Frida Olofsson

Chalmers University of Technology
Department of Microtechnology and Nanoscience – MC2
Microwave Electronics Laboratory
SE-412 96 Gothenburg, Sweden
+ 46 (0)31-772 1000

ISSN 1652-0769
Technical report MC2-466

Printed by Chalmers Reproservice
Gothenburg, Sweden 2024

Abstract

The demand for wireless communication systems with better coverage, higher capacity and lower latency grows continuously. At the same time, the number of subscribers is increasing and has already surpassed the global population. In a cellular network, a centralized macro base station is responsible to serve the users within the cell area. However, it is difficult to reach the increasing requirements by the centralized cellular architecture. Instead, distributed multiple-input-multiple-output (D-MIMO) has been proposed as a solution, where several access points or remote radio heads (RRHs) are spread out in a cell. To achieve most gain from D-MIMO the RRHs should be processed coherently, which requires radio-frequency (RF) phase synchronization among them. The hardware implementation of a D-MIMO network is non-trivial and highly dependent on the level of synchronization that is required by the particular deployment. This thesis evaluates the use of radio-over-fiber (RoF) and centralized frequency up-conversion to achieve phase synchronized RRHs in D-MIMO downlink implementations.

The first part of the thesis describes the background and motivation. Specifically, the system models for the centralized cellular base station and the D-MIMO architecture are described. The second part of the thesis explains different technologies for modulating an RF-signal onto an optical carrier using RoF: digital-radio-over-fiber (DRoF), analog-radio-over-fiber (ARoF) and sigma-delta-over-fiber (SDoF). As the need for power hungry digital-to-analog converters (DACs) is avoided in ARoF and SDoF, they are proposed as primary candidates in D-MIMO implementations. Moreover, measurement results show that SDoF is more robust than ARoF towards non-linearities in an RoF transmitter and inter-channel interference in an RoF receiver.

Finally, a SDoF architecture for D-MIMO with serially connected RRHs is presented. By connecting the RRHs in series the scalability of the system is enhanced, as one fiber link can be used to transmit signals to all RRHs. The serial connection is implemented using wavelength-division multiplexing (WDM), addressing each RRH by a specific wavelength. Through measurement results it is shown that the system with serial connection can perform similarly to one with the RRHs connected in parallel.

To conclude, this thesis presents SDoF as a fronthaul alternative for building robust, scalable and energy-efficient downlinks for D-MIMO networks. The results provide insights into the practical implementation of D-MIMO, a promising architecture for wireless communication systems.

Keywords: distributed multiple-input-multiple-output (D-MIMO), radio-over-fiber (RoF), sigma-delta-over-fiber (SDoF), optical fronthaul

List of Publications

Appended Publications

This thesis is based on work contained in the following papers:

[A] **F. Olofsson**, L. Aabel, M. Karlsson and C. Fager, "Comparison of Transmitter Nonlinearity Impairments in externally modulated Sigma-Delta-over Fiber vs Analog Radio-over-Fiber links," in *2022 Opt. Fiber Commun. Conf. and Exhibition (OFC 2022)*, Mar. 2022, pp. 6-9.

[B] **F. Olofsson**, M. Karlsson, T. Eriksson and C. Fager, "Investigation of fiber length differences in distributed MIMO Sigma-Delta-over-Fiber systems," in *49th European Conf. on Opt. Commun. (ECOC 2023)*, Sep. 2023, pp. 968–971.

[C] **F. Olofsson**, L. Aabel, T. Eriksson, M. Karlsson and C. Fager, "Sigma-Delta-over-Fiber with WDM Serial Connection for Distributed MIMO" submitted to *J. of Lightw. Technol.*, Jul. 2024.

Other Publications

The content of the following publications partially overlaps with the appended papers or is out of the scope of this thesis.

[a] L. Aabel, S. Jacobsson, M. Coldrey, **F. Olofsson**, G. Durisi and C. Fager, "A TDD Distributed MIMO Testbed Using a 1-bit Radio-Over-Fiber Fronthaul Architecture," accepted for publication in *IEEE Trans. Microw. Theory Techn.*, 2024.

[b] L. Aabel, **F. Olofsson**, H. Bao, G. Durisi and C. Fager, "Distributed MIMO Testbeds using 1-Bit Radio-over-Fiber Fronthaul," presented at *2023 Joint European Conf. on Netw. and Commun. and 6G Summit (EuCNC/6G Summit 2023)*, Jun. 2023.

Acronyms

ARoF	Analog-radio-over-fiber.
BBU	Baseband Unit.
BP-SDM	Bandpass Sigma-delta Modulation.
C-MIMO	Co-located Multiple-input-multiple-output.
CPRI	Common Public Radio Interface.
CSI	Channel State Information.
CU	Central-unit.
CWDM	Coarse Wavelength-division Multiplexing.
D-MIMO	Distributed Multiple-input-multiple-output.
DAC	Digital-to-analog Converter.
DRoF	Digital-radio-over-fiber.
DWDM	Dense Wavelength-division Multiplexing.
EVM	Error Vector Magnitude.
LO	Local Oscillator.
MU-MIMO	Multi-user Multiple-input-multiple-output.
MUX	Multiplexer.
OADM	Optical Add-drop Multiplexer.
OFDM	Orthogonal Frequency-division Multiplexing.
OSR	Oversampling-ratio.
OT	Optical Transceiver.
OTA	Over-the-air.
PA	Power Amplifier.
PD	Photodetector.
RF	Radio-frequency.
RoF	Radio-over-Fiber.
RRH	Remote-radio Head.

SDM Sigma-delta Modulation.
SDoF Sigma-delta-over-fiber.

UE User Equipment.

VCSEL Vertical-cavity Surface Emitting Lasers.

WDM Wavelength-division Multiplexing.

ZF Zero-forcing.

Contents

Chapter 1

Introduction

1.1 Motivation

The societal demand for wireless connectivity increases, and the mobile communication system has become one of the most important parts of our infrastructure. By the end of 2023, the number of mobile subscriptions worldwide was over 8 billion [1], more than the worlds total population [2]. Wireless communication is today a major part of people lives, with work meetings, courses and social gatherings just being a few examples nowadays taking place online.

As 5G is currently being implemented all over the world, we look into the 6G era, involving new use cases which put new requirements on the network. Examples of foreseen use cases are: immersive smart cities, mixed reality and consumer robots [3]. 6G is also expected to deliver trustworthiness, sustainability, limitless connectivity, accelerated automation and digitalization [4]. Hence, the ambition of what 6G will be is high, and the requirements on the mobile communication systems will increase in terms of coverage, capacity, latency and reliability. At the same time, the threat of climate change requires all major infrastructure to be resource- and energy-efficient. So, as we go into a new era with increasing demand of connectivity, the solution of using more power faces challenges. As a consequence, innovative energy efficient approaches are required.

An emerging technology that shows great prospects of both being energy efficient and improving coverage, capacity, latency and reliability is distributed multiple-input-multiple-output (D-MIMO) [5]. In contrast to a co-located multiple-input-multiple-output (C-MIMO) system shown in Fig. 1.1a where multiple antenna elements are placed together in one base station and used for beamforming, a D-MIMO system shown in Fig. 1.1b apply beamforming with elements that are distributed at different sites over a larger area. The distributed units are often referred to as access points (APs) or remote-radio heads (RRHs). Distributing the antennas reduces the spatial correlation between channels, which is beneficial for spatial multiplexing [6, Ch. 20]. It also increases the probability that a user is in the proximity of at least one RRH, allowing for lower transmit power than with one centralized base station. To conclude, D-MIMO is an innovative and energy efficient technology that provides high

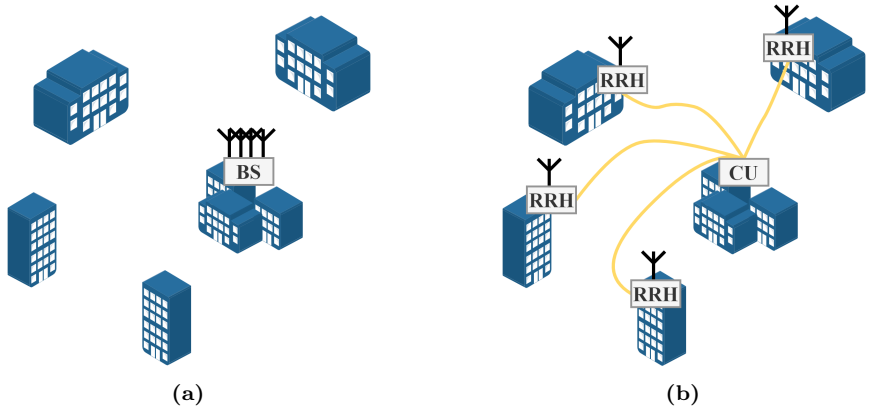

Figure 1.1: (a) Co-located MIMO with a centralized base station (BS) and four antenna elements and (b) distributed MIMO with four distributed remote radio heads (RRHs) connected to one central-unit (CU).

coverage and high capacity.

To get most gain from D-MIMO the RRHs should transmit coherently, i.e. RF phase synchronized, which is not trivial to implement in practice. This thesis addresses how to implement D-MIMO downlinks with phase-synchronized RRHs using radio-over-Fiber (RoF) fronthaul. It also evaluates the potential of using wavelength-division multiplexing (WDM) as an enabler for serial connection of the RRHs, to enhance the scalability of the system. Finally, a sigma-delta-over-fiber (SDoF) D-MIMO architecture with serially connected RRHs is presented.

1.2 Thesis Scope and Outline

Chapter 2 treats D-MIMO, starting from the basic theory behind using multiple antennas in MIMO. Thereafter, the motivation for distributing the RRHs is described in more detail; how macro-diversity can be explored to overcome challenges with shadowing and blockage. Finally, it is explained how central frequency up-conversion ensures radio-frequency (RF)-phase synchronization among the RRHs. In Chapter 3 three different RoF technologies for connecting the RRHs to a CU are presented, along with their advantages and drawbacks. Non-linearities in RoF transmitters and interference resilience in RoF receivers are then discussed, based on measurement results in [Paper A] and [Paper C]. Implementations of D-MIMO testbeds are covered in Chapter 4, which starts with a review of previous work. Based on investigations in [Paper B] and [Paper C] it is shown that the RRHs can be connected in series to enhance the scalability of the optical fronthaul, while still achieving similar communication performance as a system with RRHs connected in parallel. In the final chapter the work is summarized and potential future research directions are discussed.

Chapter 2

Distributed MIMO

Wireless communication has evolved tremendously since Marconi did the first pioneering demonstrations of wireless telegraphy in the late 19th century [7]. In the 1980s, 1G was introduced as the first standard for mobile networks, and later evolved to 2G, 3G and 4G [8]. As of today 4G is the dominant network technology, while 5G is continuously implemented at new sites.

The topology of mobile networks has changed through the different generations; in 4G systems a baseband unit (BBU) is connected to the core network through backhaul and to a RRH through fronthaul, see Fig. 2.1. The BBU, fronthaul and RRH is referred to as a base station. Each base station serves users in a specified area called a cell, hence the cellular system. It also means that each user is served by one base station at a time, and when a user moves from one cell into another, a handover to another base station has to be done. The network topology for 5G is similar, but splits the BBU into two units and introduces a midhaul between them [9]. Regardless, the approach of having one base station per cell remains in 5G. The early generations of mobile communication used single antennas at both the base stations and the users. However, when Foschini showed in [10] the large capacity improvement that could be achieved when using multiple antennas at the transmitter and receiver, it sparked a growing interest in multi-antenna communication.

This chapter describes the fundamentals of mimo communication, and how it can be used to increase capacity, coverage and robustness in a wireless communication system. The chapter also explains the background and arguments for exploring D-MIMO systems, instead of C-MIMO system, and what new implementation challenges that causes.

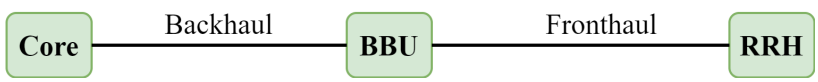

Figure 2.1: Network structure for 4G including: core, backhaul, baseband unit (BBU), fronthaul and remote radio head (RRH).

2.1 Multiple-Input-Multiple-Output

In mimo technology multiple antenna elements are used for signal transmission and reception, and it is today implemented in most wireless communication systems. When using multiple transmit and receive antennas, a signal will propagate on several statistically de-correlated channels, and so called spatial diversity is created. Spatial diversity increases robustness and reliability, by counteracting fading in the wireless channel [6, Ch. 13]. Fading is temporal and spatial variations of the received signal power, which degrades the throughput. A distinction is made between large-scale and small-scale fading. Large-scale fading refers to path loss due to the propagation distance in the air as well as shadowing when objects block the way between the transmitter and the receiver. Small-scale fading refers to time variations in the channel, due to multipath or Doppler spread. If not managed properly the system capacity will be degraded [6, Ch. 13].

Apart from creating diversity, using multiple antennas also makes it possible to apply beamforming. Beamforming means to control the overall radiation pattern from several antenna elements, by managing the phases of the signals transmitted from each separate element. For example it can be used to focus the transmitted energy at a certain location, hence increase the signal strength there. In mimo systems, beamforming is commonly applied based on channel state information (CSI); CSI refers to knowing the channel response between the transmitter and receiver [6, Ch. 20]. CSI can both be used to precode the signals at the transmitter and post-combine the signals at the receiver.

Typically, known orthogonal pilot sequences are used to estimate the response of the channel between each pair of antennas, also called channel estimation. Orthogonality of pilots can be achieved using different methods, for instance: time-, frequency- or code-orthogonality. Assuming the channel is reciprocal and the uplink and downlink use the same frequency band, pilot transmission can be performed in either direction. For pilot transmission in the downlink, the user does the channel estimation, and in the uplink, the base station does the channel estimation. The advantages of letting the user do the channel estimation is faster feedback and adaptability to each user, but it leads to more complex and power hungry user equipment (UE). Doing channel estimation in the uplink relaxes the requirements on the UE, and often provides more accurate CSI as the base stations have better hardware, more antennas and computational resources. In a realistic system hardware differences between the uplink and downlink exist, and reciprocity calibration has to be performed [11].

Mathematically we can describe the mimo channel with a matrix $\mathbf{H}$, of dimension $R \times T$; R is the number of receive antennas and T the number of transmit antennas. The received signal $\mathbf{y}$ has the dimension $R \times 1$ and becomes

$$\mathbf{y} = \mathbf{H}\mathbf{x} + \mathbf{w}, \tag{2.1}$$

where each row of $\mathbf{y}$ corresponds to the signal at each receiving antenna element, $\mathbf{x}$ corresponds to the transmitted signal of dimension $T \times 1$ and $\mathbf{w}$ represents additive noise. Beamforming is implemented by precoding the signals to transmit. The simplest case of precoding is to choose a precoder matrix $\mathbf{P}$ such that it cancels out the effect of $\mathbf{H}$, i.e. zero-forcing (ZF). The

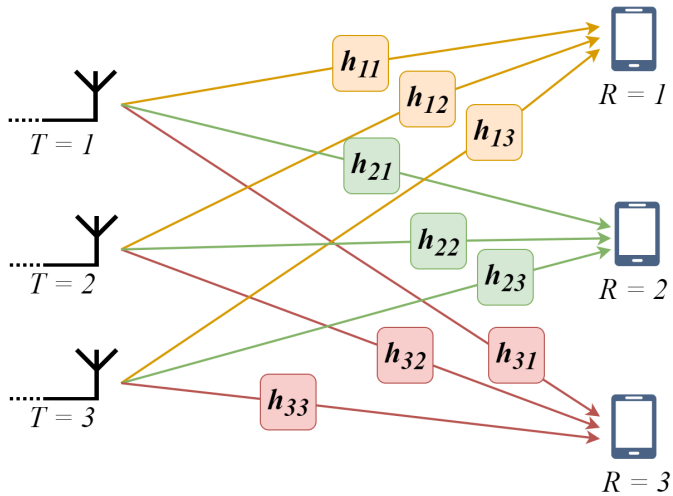

Figure 2.2: Illustration of how multiple antennas at the transmitter are used to serve multiple users. Note that in a multipath environment the channel paths will not be straight beams.

ZF-precoder is constructed from the channel estimate $\hat{\mathbf{H}}$ using the Moore Penrose pseudo-inverse [6, Ch. 20], according to:

$$\mathbf{P}_{\text{ZF}} = \hat{\mathbf{H}}^{\text{H}}(\hat{\mathbf{H}}\hat{\mathbf{H}}^{\text{H}})^{-1}. \tag{2.2}$$

ZF-precoding will also result in spatial multiplexing, where multiple independent data streams between the transmitter and receiver are created, which effectively increases the capacity of the system. We define the transmitted signal without precoding as $\tilde{\mathbf{x}}$ and the precoded transmitted signal as $\mathbf{x} = \mathbf{P}\tilde{\mathbf{x}}$, where $\mathbf{P}$ is the precoder matrix of dimension $T \times R$ and $\tilde{\mathbf{x}}$ has the dimensions $R \times 1$. Many other precoders than ZF exist, which are optimized for other objectives. One example is the maximum-ratio-transmission precoder, which maximizes the achieved SNR at the receiver [12].

In the case imagined so far all receiving antennas are located together, but beamforming can also be used to serve multiple receiver antennas located at different users. If all users are equipped with a single antenna, R different users can be served. If ZF-precoding is applied in a multi-user scenario, inter-user-interference is minimized as the precoding creates a radiation pattern with maximas at the intended user location and nulls at the other users locations, for each user respectively. As a consequence each user only receives its corresponding data stream, also achieving spatial multiplexing. An illustration of spatial multiplexing in multi-user multiple-input-multiple-output (MU-MIMO) is shown in Fig. 2.2. However, it should be emphasized that in a multipath scenario the paths between each transmitting and receiving antenna is not a straight beam as illustrated in the figure.

2.2 Co-located and Distributed MIMO

As mentioned in the previous section, spatial diversity can be used to combat fading in the wireless channel. Spatial diversity for managing large-scale fading is referred to as macro-diversity, and gave rise to the idea of D-MIMO. In D-MIMO the antennas are spatially distributed over a large area, shown in Fig. 1.1b. As mentioned in the introduction, the distributed units in D-MIMO are often referred to as access points or RRHs. The RRHs are connected to a central-unit (CU) where processing is done. In [13] and [14] a system with 12 distributed RRHs was compared to one where all were placed at one site, showing the strength of D-MIMO in combating shadowing by walls etc. The measurement results in [14] were also compared to ray-tracing simulations in [15]. Apart from providing more uniform coverage, D-MIMO is also a foundation for the promising technology of cell-free massive mimo that was proposed in [16], where the concept of a cell is discarded. Instead all RRHs serve all users, avoiding challenges such as low power to users on the edge between two cells, inter-cell interference etc. [17].

D-MIMO can be implemented with different processing capabilities in the CU and RRHs, as well as different level of cooperation between the RRHs. In [18] the amount of cooperation between RRHs in uplink operation was theoretically investigated, and the result showed that centralized signal processing allowing for full level of RRH cooperation gave the highest spectral efficiency. To achieve maximum gain from a D-MIMO system the RRHs should also be operated coherently, which requires highly accurate phase synchronization among them [19]. Consequently, perfectly phase synchronized RRHs is assumed in many theoretical studies on D-MIMO [17, 18]. However, implementing phase synchronized distributed RRHs in real hardware is not trivial.

The challenges of synchronizing distributed RRHs can be understood by looking at how a conventional radio operates; analog baseband signals are mixed with an RF-signal generated by a local oscillator (LO), which creates a modulated signal at RF-frequency carrier to transmit over-the-air (OTA), see Fig. 2.3a. Due to the proximity of the antenna elements in C-MIMO systems the same LO can be used to up-convert all the signals, automatically ensuring phase synchronization, see Fig. 2.3b. But in a system with several distributed RRHs using one mixer and LO at each site and at the same time ensuring phase synchronization is not feasible.

Different solutions for implementing distributed phase-synchronized RRHs have been proposed: using independent LOs at the RRHs and distributing a

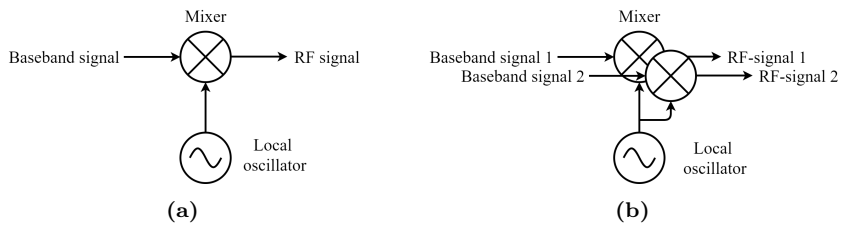

Figure 2.3: Analog up-converison from baseband signal to RF-signal using a mixer and a local-oscillator in a (a) single-antenna system and a (b) co-located multi-antenna system.

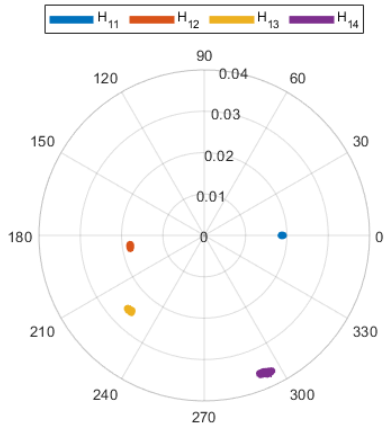

Figure 2.4: Estimation of the channel coefficients through 70 consecutive measurements using four remote radio heads (RRHs) [Paper C]. The phase of the channel coefficients represents the relative phase between each RRH.

clock reference over the fronthaul [20, 21], transmitting clock references between the RRHs over-the-air [22] or doing analog or digital frequency up-conversion centrally in the CU and transmit the RF-signals directly over the fronthaul [13, 23–25]. The latter is an interesting solution as it ensures synchronization without further operations in the RRHs. We showed in [Paper C] that four phase synchronized RRHs could be implemented with digital central frequency up-conversion. Fig. 2.4 shows 70 consecutive OTA measurements of the relative RF-phase between the transmitted signals from the four RRHs. During all measurements the relative phase is stable, indicating phase synchronization among the RRHs. However, transmitting RF-signals—and not baseband signals—over the fronthaul changes system requirements, compared to previous standards. To implement it in a real D-MIMO system, different fronthaul solutions have to be assessed.

2.3 Chapter Summary

In this chapter the evolution of mobile networks was described. Moreover, it was explained how using multiple antenna elements for transmitting and receiving introduce diversity and beamforming capabilities in a system. Finally, the chapter covered the arguments for using D-MIMO instead of C-MIMO, to create macro-diversity and combat large-scale fading. In the next chapter RoF will be presented as a fronthaul candidate for connecting phase-synchronized RRHs to a CU in D-MIMO systems.

Chapter 3

Radio-over-Fiber Optical Fronthaul

Optical fiber cables are widely used in today's communication systems, due to their low loss and large bandwidth. The standard protocol for fronthaul transmission in 4G is to use digital baseband signals and the common public radio interface (CPRI) (later developed to enhanced-CPRI) protocol [26]. In the RRH, digital-to-analog converters (DACs) then convert the digital CPRI bitstream to an analog signal, which is up-converted to RF-frequencies using an analog mixer and local oscillator. In the previous chapter is was shown that synchronizing independent local oscillators in each spatially distributed RRH is a challenge, but that phase synchronization is automatically ensured if frequency up-conversion is done centrally in the CU, and RF-signals are transmitted over the fronthaul.

Combining the concept of optical fiber-based fronthaul with central frequency up-conversion and direct transmission of RF-signals from the CU results in the idea of RoF fronthaul. Note that a distinction is made here between RoF where the RF-signal is transmitted over the fiber, and other variants where either an intermediate- or baseband signal is transmitted over the fiber—which require up-conversion in the RRH.

For backhaul, RoF has been investigated for a long time, due to its large bandwidth and ability to support high-frequency signal transport [27]. Recently, interest has increased for also using RoF fronthaul in D-MIMO networks, due to the inherently phase synchronized RRHs. In this chapter the three most common RoF technologies are introduced: digital-radio-over-fiber (DRoF), analog-radio-over-fiber (ARoF) and SDoF. Also a summary of the optical hardware used for transmission and reception in RoF links along with a comparison of ARoF and SDoF is presented, based on [Paper A] and [Paper C].

3.1 Digital-Radio-over-Fiber

Fig. 3.1a shows the schematic of a typical DRoF link. In DRoF a digital serialized representation of the modulated RF-signal is transmitted over fiber and recovered at the RRH using a photodetector followed by a DAC [28]. One

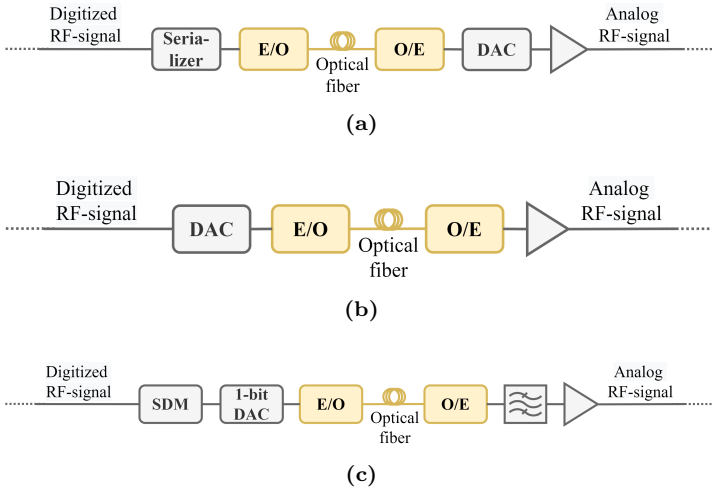

Figure 3.1: (a) Digital-Radio-over-Fiber link including: serializer, electrical-to-optical (E/O) conversion, optical-to-electrical (O/E) conversion, digital-to-analog converter (DAC) and amplifier. (b) Analog-Radio-over-Fiber link including: DAC, E/O conversion, O/E conversion and amplifier. (c) Sigma-Delta-over-Fiber link including: sigma-delta modulator (SDM), 1-bit DAC, E/O conversion, O/E conversion, bandpass filter and amplifier.

advantage with DRoF is its robustness towards non-linearities in the optical components, resulting from its binary nature. However, by digitizing the frequency up-converted RF-signal—and not the baseband signal—high sample rate and high resolution DACs are needed, which comes with increased cost and power consumption [29]. The requirements on the DACs can be decreased to some extent by using direct bandpass sampling of the signal, where a sample rate lower than the Nyquist rate is used intentionally [30]. But even though bandpass sampling can lower the sample rate requirement to some extent it can not remove it completely, and DACs remains the components that limit performance in DRoF systems [31]. As the expected number of RRHs in D-MIMO is large, the scalability of DRoF is questionable due to the need of high sample rate and high resolution DACs.

3.2 Analog-Radio-over-Fiber

In Fig. 3.1b the schematic of a typical ARoF link is presented. In ARoF the RF-signal is directly modulated onto the optical carrier, using either a directly modulated laser or an external optical modulator [32, Ch. 6]. The signal is transmitted over the fiber link and recovered at the RRH using a photodetector.

ARoF allows for simple RRHs as only a photodetector and a power amplifier (PA) is required (no DAC) but requires high bandwidth and large dynamic range lasers, photodetectors and modulators. Under the assumption that components with sufficient bandwidth are available, ARoF allows for higher bandwidth efficiency than DRoF [33]. Another advantage with ARoF is that so called optical heterodyning or frequency up-conversion can be used to achieve higher carrier frequency of the RF-signal [34]. Then two optical tones of different wavelengths are mixed in a photodetector to create a high frequency RF-signal

without needing high sample rate in the CU [35].

ARoF is an interesting candidate for D-MIMO implementations due to its simple design of RRHs and high bandwidth efficiency [24]. However, despite its many advantages ARoF is sensitive towards non-linearities in the optical components, which limits the dynamic range [Paper A], [36].

3.3 Sigma-Delta-over-Fiber

In Fig. 3.1c the schematic of a typical SDoF link is presented. In SDoF the RF-signal is quantized with few bits, which creates a low resolution representation of the original signal to be modulated onto the optical carrier. However, when quantizing a signal with very few bits a large quantization error occurs, and the original signal is distorted. In sigma-delta modulation (SDM) oversampling and noise shaping techniques are used to minimize the in-band quantization error. The oversampling lowers the power per frequency of the quantization error by spreading it over a wider spectrum. The noise-shaping shapes the quantization error to be minimized within a specified frequency band—the passband. As a consequence, the original signal can be recovered by bandpass filtering the sigma-delta modulated signal, with a low level of in-band quantization noise [37, Ch. 1].

In two-level SDoF binary signals are transmitted over the optical fronthaul, which lowers the requirements on DACs as well as optical components [38]. Specifically: 1-bit DACs and digital optical components can be used, while the signal still can be recovered in the RRHs by bandpass filtering. The use of 1-bit communication also makes it possible to take advantage of the large development in low-cost and high-speed digital optical interconnects for data centers.

The oversampling-ratio (OSR) in SDM is defined as

$$\mathrm{OSR} = \frac{f_s}{2B}, \tag{3.1}$$

where f_s is the sampling frequency and B is the bandwidth of the modulated RF-signal [37, Ch. 1]. The noise-shaping is applied using feedback loops where the output from the quantizer is feed back to the input through an integrator, working as a filter. It is this process that pushes the the error created in the low resolution quantization out of the band of interest. The order of the SDM defines how many integrators there are in the noise-shaping feedback loop [37, Ch. 1].

SDoF allows for simple RRHs without DACs—just as ARoF—while being resilient towards non-linearities in the optical domain—just as DRoF—at the cost of high oversampling in the CU. Therefore, SDoF is considered a compromise between ARoF and DRoF, and a promising candidate for implementing D-MIMO [13, 23, 25, 38].

3.4 ARoF versus SDoF

In the previous section three RoF technologies for connecting the CU to the RRHs in D-MIMO networks were described: DRoF, ARoF and SDoF. However,

as future D-MIMO systems are expected to consist of a large number of RRHs, scalability is crucial. So even though DRoF has certain advantages, the need of complex and power hungry DACs in the RRHs makes it more challenging to scale up the number of RRHs, than with ARoF and SDoF. Therefore the focus in this section is on ARoF and SDoF.

The performance of an RoF link depends on both the transmitter doing electrical-to-optical conversion and the receiver doing optical-to-electrical conversion. For both RoF transmitter and RoF receiver, different choices of hardware and how to operate it can be made. In this section we discuss different hardware solutions for RoF transmitters and receivers. We also make comparisons between ARoF and SDoF links in terms of robustness towards non-linearities and inter-channel interference, based on the results in [Paper A] and [Paper C].

3.4.1 Linearity in the RoF Transmitter

Either directly modulated lasers or external modulators can be used to modulate an RF-signal onto an optical carrier. In a directly modulated laser the electrical signal modulates the output light of the laser, with the advantage of a small footprint. Especially vertical-cavity surface emitting laserss (VCSELs) have received a lot of attention due to their low manufacturing cost and simplicity in wafer-scale testing. In external modulation, the output light from a continuous wave laser is passed through an optical modulator, which alters the phase and/or amplitude of the optical signal based on an input electrical signal. External modulation generally offers higher bandwidth, higher quality modulation and allows for building more complex transmitters, but are considered bulky compared to directly modulated lasers. Both SDoF and ARoF can be implemented using either external or direct modulation.

In [Paper A] we investigated ARoF and SDoF links in terms of the sensitivity towards non-linearities in an external optical modulator. An intensity modulator of Mach-Zehnder type was biased at the quadrature point and the input power was swept for both SDoF and ARoF. In Fig. 3.2 the transfer function

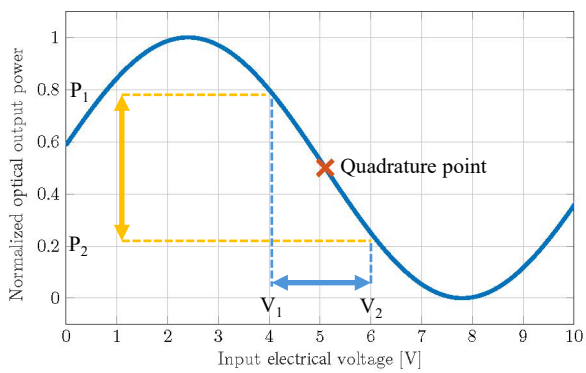

Figure 3.2: Transfer function from electrical input voltage to normalized optical output power for an intensity modulator. The red cross marks the bias point of the modulator. V_1 and V_2 corresponds to the maximum and minimum input voltage, and P_1 and P_2 to the corresponding output optical power.

from electrical input voltage to optical output power for an optical intensity modulator is presented. The quadrature point is marked, around which the input and output vary. The modulator transfer function is approximately linear in a regime close to the quadrature point, hence the electrical input voltage can not be too high. However, the electrical input voltage level translates to the optical output power from the modulator, and there is a trade-off between the non-linearity and the amplitude of the optical modulation. In SDoF, the input signal to the modulator consists of two levels (representing a 0 or 1), which corresponds to moving between the two points V_1 or V_2 in the transfer function. In ARoF the input signal to the modulator is a multi-level representation of a continuous signal, hence it corresponds to many different values on the transfer function between between V_1 or V_2.

Even though a sigma-delta modulated signal is a binary signal, the shape of the spectrum is important and it is interesting to investigate how that is affected when operating the modulator in the nonlinear regime. In Fig. 3.3a the measured error vector magnitude (EVM) versus the power of the input peak voltage for SDoF and ARoF and four different modulation orders (QPSK, 16QAM, 64QAM, 256QAM) is presented. In the measurements a 2.35 GHz single-carrier signal with 40 MBd symbolrate was used. For SDoF the RF-signal was sigma-delta modulated using a fourth order sigma-delta-modulator with 10 GS/s sample rate.

The measurements show that external modulators can be driven with a higher peak voltage when using SDoF compared to ARoF, resulting in a lower EVM. In the constellation diagram presented in Fig. 3.3b for a peak power of $P_{\text{in, peak}} = 17.8$ dBm, it is noted how the ARoF implementation is more severly affected by the non-linearities in the modulator than SDoF. However, in Fig. 3.3a it is shown that for high input peak voltage SDoF also gets effected by non-linearities and EVM increases, indicating that despite its binary nature SDM does not behave exactly as digital modulation. To conclude, the results in [Paper A] showed that the binary nature of SDM makes SDoF less sensitive towards non-linearities in an external optical modulator than ARoF. A similar study was done in [36] with directly modulated VCSELs also showing that ARoF was more sensitive to non-linearities than SDoF.

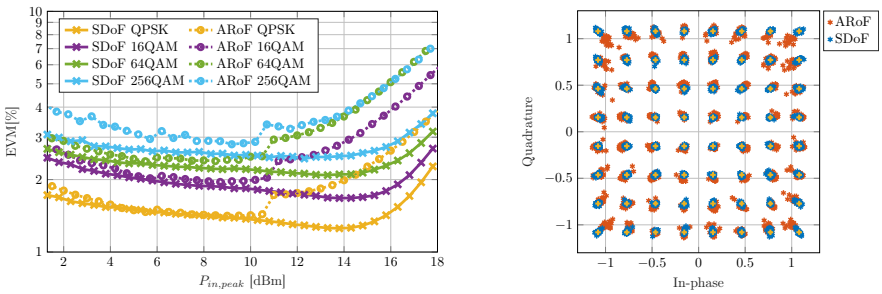

(a) **(b)**

Figure 3.3: Measurement results comparing analog-radio-over-fiber (ARoF) and sigma-delta-over-fiber (SDoF) in terms of sensitivity towards non-linearities in an optical intensity modulator. (a) Measured error vector magnitude (EVM) for four different QAM modulation orders and (b) constellation diagram at the higher peak power = 17.8 dBm [Paper A].

3.4.2 Interference in the RoF Receiver

After transmission over the optical fiber the signal is converted back to electrical domain in the RRH. It can be done using a photodetector, which is a square law detector that outputs a current based on the input optical power—or intensity. The electrical output current i_{el} also depends on the responsivity R of the detector and is given by

$$i_{\text{el}} = RP_{\text{opt}}, \tag{3.2}$$

where P_{opt} is the optical input power to the detector. The responsivity of a photodetector depends on several parameters such as material, wavelength, quantum efficiency etc. [32, Ch. 8].

For ARoF the continuous amplitude variations of the RF-signal have to remain when converting from optical to electrical domain. For SDoF only two levels are required when converting, which makes it possible to use digital low-cost optical interconnects. As these devices are designed for transmission and reception of digital signals they operate in a binary mode, and apart from a photodetector also include other circuitry such as amplifiers and comparators.

In [Paper C] we investigated the receiving part of an optical transceiver (OT), by measuring its output electrical power as well as the EVM for a SDM signal transmitted over the link for different average optical input power, see Fig. 3.4. The average electrical output power is not a linear function of the average optical input power, but rather a step function. This is attributed to that the OT is designed to operate with digital signals, hence only two signal levels. The average output power remains at −12 dBm for all average optical input power above −24 dBm, but the EVM improves until the average optical input power is above −15 dBm. The measurement results confirm that the OT operates non-linearly and includes more components than a photodetector. The measurement results also specifies that to achieve acceptable EVM, this specific OT should be operated with optical input power larger than −15 dBm.

In [Paper C] we also investigated how SDoF and ARoF compare in terms of resilience towards optical interference between channels. Two WDM channels were modulated with either analog signals or SDM signals, and combined using an optical multiplexer (MUX), where one was treated as an interferer.

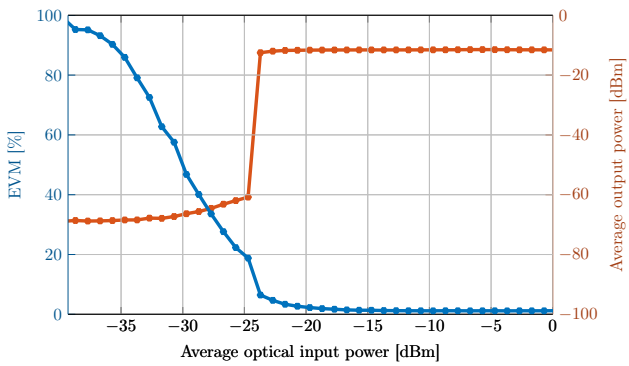

Figure 3.4: Measured average electrical output power and error vector magnitude (EVM) of an optical transceiver (OT) for different average optical input power [Paper C].

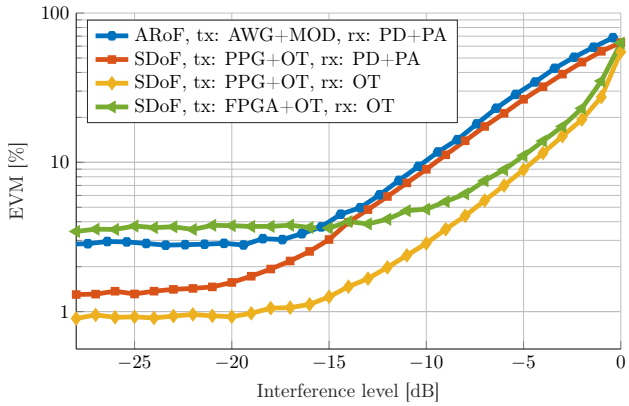

Figure 3.5: Measured error vector magnitude (EVM) for different interference levels, for ARoF and SDoF [Paper C]. Four different configurations of transmitter (tx) and receiver (rx) are used including: arbitrary waveform generator (AWG), intensity modulator (MOD), photodetector (PD), power amplifier (PA), pulse pattern generator (PPG), optical transceiver (OT) and field-programmable gate array (FPGA).

As RoF receiver for the SDoF implementations both {photodetector (PD)+PA} and OT were used. In ARoF implementations the OT can not be used as receiver, due to its non-linearity, hence only {PD+PA} was used. In summary, the measurements included four different configurations of transmitting and receiving hardware, where the most important difference was whether an OT or {PD + PA} was used as receiver.

In Fig. 3.5 the measured EVM of the received symbols is presented versus level of interference. It can be noted that the setups using SDoF with OT as receiver is more resilient towards optical interference, than both ARoF and SDoF using {PD + PA}. The results show that using low-cost optical interconnects in SDoF not only enhances scalability but also makes the system more resilient towards inter-channel interference.

3.5 Chapter Summary

In this chapter three technologies for transmitting frequency up-converted RF-signals over fiber were presented, and their advantages, disadvantages and implementation scalability were discussed. ARoF and SDoF were compared in terms of non-linearities in an external optical modulator as well as sensitivity towards inter-channel interference. Measurement results from [Paper A] and [Paper C] showed that SDoF is more robust towards non-linearities and inter-channel interference than ARoF. In next chapter a D-MIMO SDoF architecture with serially connected RRHs using WDM will be presented and discussed.

Chapter 4

D-MIMO with Radio-over-Fiber

The previous chapters discussed the motivation for implementing D-MIMO with optical fronthaul and centrally frequency up-converted RoF. It also showed how SDoF, due to its binary nature, has certain advantages compared to ARoF in terms of being more robust towards non-linearities and inter-channel interference.

This chapter regards how RoF can be used to implement D-MIMO testbeds, starting with a review of previous experimental work. The chapter also discusses how connecting the RRHs in series instead of in parallel, using WDM, enhances the scalability of the system. Finally, an experimental demonstration of a SDoF architecture with four serially connected RRHs based on the work in [Paper C] is presented.

4.1 D-MIMO RoF Testbeds

It is important to build and investigate D-MIMO testbeds, to asses how different hardware implementations compare and to create test environments for algorithms, signal processing etc. D-MIMO testbeds have been demonstrated with various fronthaul technologies [39–42]; however, this thesis focuses on implementations using ARoF or SDoF fronthaul. The focus is also on downlink transmission.

4.1.1 ARoF Implementations

As already mentioned in Section 3.2 ARoF is an established technology for fronthaul links connecting to one single base station or RRH [43], which makes it interesting to use it for connecting several distributed RRHs. In [24] ARoF D-MIMO measurements were presented using two phase coherent RRHs, showing a 5.3 dB gain (close to the theoretical value of 6 dB) when performing phase-coherent transmission from the two RRHs, compared to when transmitting from one RRH alone. One RRH was connected to the CU using an ARoF link and one using a coaxial cable. Both RRHs transmitted at a carrier frequency

622 MHz. Similar work was done at millimeter-wave (mm-wave) frequencies in [44], with two RRHs transmitting at a carrier frequency of 26.5 GHz. Phase synchronization was ensured by doing central frequency up-conversion in the CU, which for mm-wave puts higher requirements on the bandwidth and sample rate of signal generators and lasers, compared to sub-6 GHz demonstrations. The measurement results showed that the bitrate could be increased from 24 Gb/s to 48 Gb/s with coherent transmission.

Another approach that was demonstrated in [35], is to transmit the signal at a lower frequency from the CU, and create the mm-wave carrier using optical frequency mixing in a photodetector at the RRH. This allows the requirements on the hardware in the CU to be relaxed compared with using central frequency up-conversion. Two RRHs with 60 GHz carrier frequency were implemented and used to transmit phase-coherently to a user. For a 2 Gb/s 4-QAM signal an improvement in receiver sensitivity of 1.8 dB was shown, compared to when not transmitting coherently from the RRHs. Similar work with phase-coherent transmission from two RRHs and optical mixing was presented in [45], including a theoretical derivation of the gains acquired from coherent transmission.

Another alternative is intermediate-frequency-over-fiber (IFoF), where a lower carrier frequency is transmitted over the fiber and up-converted electrically at the RRH. IFoF requires electrical up-conversion in the RRHs, hence the phase-synchronization among the RRHs is not automatically ensured and needs to be carefully considered. In [46] IFoF with four RRHs was demonstrated, which included a clock signal in the fiber transmission for phase synchronization and provided data-rates up to 9 Gb/s.

4.1.2 SDoF Implementations

Experimental work on SDoF has also been done, demonstrating both single link [47,48] and D-MIMO testbeds. In [13] a SDoF D-MIMO testbed was presented, supporting up to 12 RRHs transmitting at an RF-frequency of 2.35 GHz with bandwidths up to 100 MHz. Digital up-conversion to RF-frequency and SDM were done offline in MATLAB and the sigma-delta modulated bits were uploaded to an FPGA, that together with a computer served as CU. A similar demonstration with two RRHs was done in [23], with the main difference that the SDM and frequency up-conversion were implemented on the FPGA, allowing for real-time processing.

SDoF testbeds are considered especially beneficial in the sub-6GHz frequency band, as it makes it feasible to sigma-delta modulate the RF-signal directly. However, demonstrations at mm-wave have been done, but require more complex schemes or up-conversion in the RRHs. In [21] mm-wave transmission at 24-28 GHz RF-frequency from two RRHs was shown, supporting one user with 160.32 MHz bandwidth. A SDM signal at an intermediate frequency of 2.5 GHz transmitted the data from the CU to the RRHs, where the signal was up-converted to mm-wave using a clock and data recovery module to create a reference for synchronization from the optical transceiver clock signal. Another demonstration at 26.5 GHz carrier frequencies with two RRHs was done in [20], successfully supporting two users with up to 748 MHz bandwidth using spatial multiplexing. The signal was up-converted in the RRHs using mixers and an over-fiber transmitted periodic bitstream as LO.

4.2 WDM Serial Connection

All experimental work described in the previous section used one optical fiber cable per RRH, but it becomes impractical as the number of RRHs are expected to increase substantially in D-MIMO networks. A way to enhance scalability of the optical fronthaul is to connect the RRHs in series as shown in Fig. 4.1a, instead of in parallel as shown in Fig. 4.1b. A theoretical discussion of using serial connection to enhance scalability in systems with a large number of RRHs was presented in [49], based on the radio stripes concept proposed in [50]. In a radio stripe the serial connection is done by creating multiple channels in one electrical cable.

For RoF fronthaul, WDM can be used to create multiple channels based on different wavelengths. In coarse wavelength-division multiplexing (CWDM) the standardized wavelength spacing is 20 nm, allowing for 18 wavelengths in total [51]. In dense wavelength-division multiplexing (DWDM) the wavelength spacing is smaller, and more channels can be implemented in the same fiber, but it is potentially more sensitive to inter-channel interference [52].

WDM has already been shown feasible to provide signals to separate antenna elements or base stations using ARoF. In [53], different wavelengths were used to provide signals to the different elements of a co-located antenna array, and beamforming was controlled from the CU. Similarly, a 2×2 C-MIMO setup was presented in [54], where two different wavelengths were used to serve the two transmitting antennas. In [55], instead the different wavelengths were used to serve four independent antennas placed in one base station and covering one 90° sector each. The use of WDM for optical serial connection was demonstrated in [56], where two distributed antenna units were served by different wavelengths, but the antenna units did not transmit coherently. At each site a coupler and a de-multiplexer isolated and dropped the correct wavelength. In [57] the concepts of optical serial connecting and coherent transmission were discussed. ARoF with WDM was proposed as a solution for connecting a CU to two distributed antenna units, that would transmit coherently to the UEs in one cell. However, the distributed antenna units that would transmit coherently were not proposed to be located on the same serial stripe, but at different stripes at the same distance from the CU. No work on serially connected RRHs using SDoF has been demonstrated.

Figure 4.1: Distributed MIMO system with (a) serially connected and (b) parallel connected remote radio heads (RRHs) [Paper C].

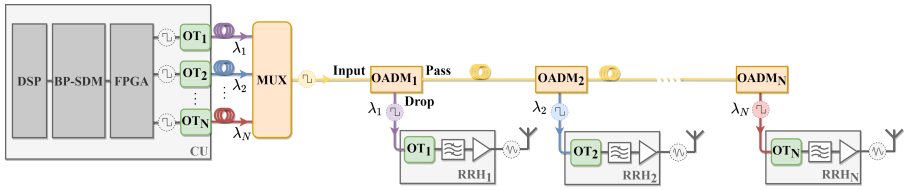

Figure 4.2: Schematic of the SDoF architecture with N remote radio heads (RRHs) connected in series using WDM [Paper C]. In the central unit (CU) digital signal processing (DSP) and bandpass sigma-delta modulation (BP-SDM) is done. The output bitstream is written to the field-programmable-gate-array (FPGA) that is connected to four transmitting optical transceivers (OTs) of different wavelength. The optical signals are combined in an optical multiplexer (MUX) and transmitted over fiber. At each RRH one signal is dropped using optical-add-drop-multiplexers (OAMDs) and inserted to a receiving OT. The output electrical signal from the OT is bandpass filtered to recover the original RF-signal, amplified with a power amplifier (PA) and transmitted over-the-air with a patch antenna.

4.3 SDoF WDM Architecture

We investigated in [Paper C] a D-MIMO SDoF downlink architecture with WDM serial connection of the RRHs. It could also be extended to uplink using the concept presented in [25]. A schematic of the proposed architecture is presented in Fig. 4.2 with N RRHs. The architecture uses the OTs discussed in Chapter 3 for electrical-to-optical conversion in the CU and optical-to-electrical conversion in the RRHs.

The CU consists of a computer, an FPGA and N OTs. Digital-signal-processing (DSP) includes: generating QAM-symbols in Matlab, pulse shaping and up-converting them digitally to a carrier frequency of 2.35 GHz. Bandpass sigma-delta modulation (BP-SDM) is then applied to the RF-signal, creating a bitstream. When transmitting pilots, the RRHs are assigned with time-orthogonal 16-QAM sequences. When transmitting data, one 16-QAM sequence per user is created and mapped to the number of RRHs by precoding. The N SDM bitstreams are written to the FPGA, which connects to N OTs that do electrical-to-optical conversion. The optical output signals from the OTs are combined into one fiber using an optical MUX.

At each RRH one optical wavelength signal is dropped using an optical add-drop multiplexer (OADM), while the others are passed through. In Fig. 4.3 the spectrum at the input and two output ports (drop and pass) of a 1570 nm OADM is shown. The drop port has high isolation, as the spectrum only includes the signal of the wavelength aimed to be dropped. At the output signal from the pass port all wavelengths are seen, but with significantly lower power in the wavelength that is supposed to be dropped and not passed (1570 nm).

The output from the OADM drop port is inserted to the RRH where the optical signal is converted to electrical using an OT. The electrical output signal from the OT is bandpass filtered to convert the bitstream to the original RF-signal, amplified and transmitted over-the-air with a patch antenna.

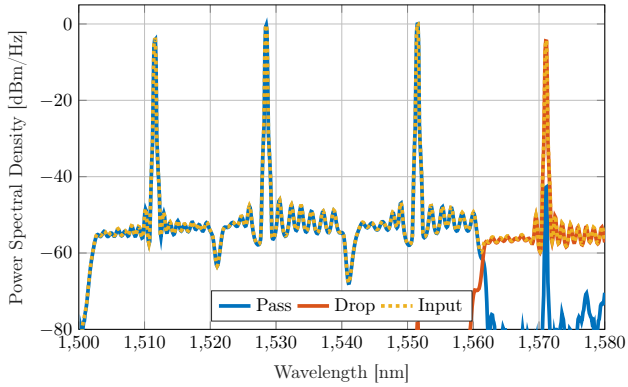

Figure 4.3: Optical spectrum at the input and two output ports of the 1570 nm optical add-drop multiplexer (OADM) [Paper C].

4.4 Different Fiber Lengths

A fundamental challenge that arise when connecting RRHs in series is that the fiber length from the CU to each one of them will be different. The difference in length will result in different propagation time to each RRH as well as different optical input power. The optical loss increases with fiber length as well as the number of OADMs that a signal passes, hence the RRH furthest away from the CU will receive lowest input power.

4.4.1 Time Delay Compensation

The time delay differences cause the signals to arrive at the user out of time synchronization, and the precoding to not function as intended. This is similar to how different wireless signal path components arrive at different times in a multipath propagation environment, where orthogonal frequency-division multiplexing (OFDM) often is used to minimize the effect. OFDM was first proposed in [58] and is a digital modulation technique where a wideband signal is divided into a number of narrowband sub-carriers, to create a flat frequency response within each small bandwidth [59].

In [60] the effect of different fiber length to each RRH was investigated, using OFDM signals. Measurement results showed that by using OFDM and symbol rates of 250 kHz the EVM remained constant for fiber length differences up to 100 m. However, to support larger bandwidths and larger differences in fiber lengths, and as the length differences for the serially connected RRHs are fixed, the effect can be calibrated away.

In [Paper B] we investigated this effect using two RRHs connected in parallel with fibers of different length. Single-carrier modulation was used, to explore the fundamental limits with different path lengths when not managed using OFDM. Time delay compensation was done by delaying the signal to the RRH furthest away with the theoretical propagation time difference in the fiber [24] according to,

$$\tau \approx \frac{n\Delta L}{c_0}, \tag{4.1}$$

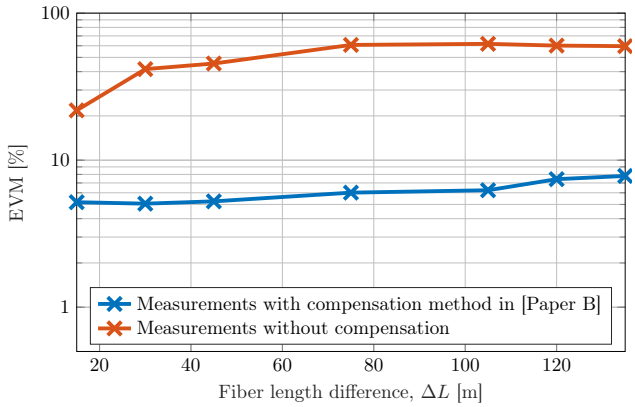

Figure 4.4: Measured error vector magnitude (EVM) versus fiber length difference between two remote radio heads (RRHs) [Paper B]. Compensation refer to the proposed time delay compensation method.

where n is the group index, c_0 the vacuum light velocity and ΔL the difference in fiber length between the two RRHs. In Fig. 4.4 the measured EVM of the received symbols versus fiber length difference is shown, for measurements with and without applying time delay compensation. With time delay compensation EVM remains at a low level as the fiber length difference increases, and without it is severely degraded.

In the system with parallel connected RRHs, the theoretical approximation resulted in an acceptable EVM, but when adding a MUX and OADMs that introduce additional delays, more precise compensation is needed. In [Paper C] we therefore extended the time delay compensation method and instead of using the theoretical approximation we measured the time-delay as an initial calibration step in the measurement procedure. Time orthogonal pilot sequences were transmitted over-air from the RRHs, and received with a patch antenna connected to an oscilloscope. The delay was estimated by cross correlating the transmitted and received signals, using the signal to the furthest RRH as a reference. The compensation was done by delaying the RF-signals before SDM for each RRH in the opposite order, hence the signals to all RRHs were delayed except for the one furthest away. To calibrate fractional delay, both delay estimation and compensation were applied in frequency domain.

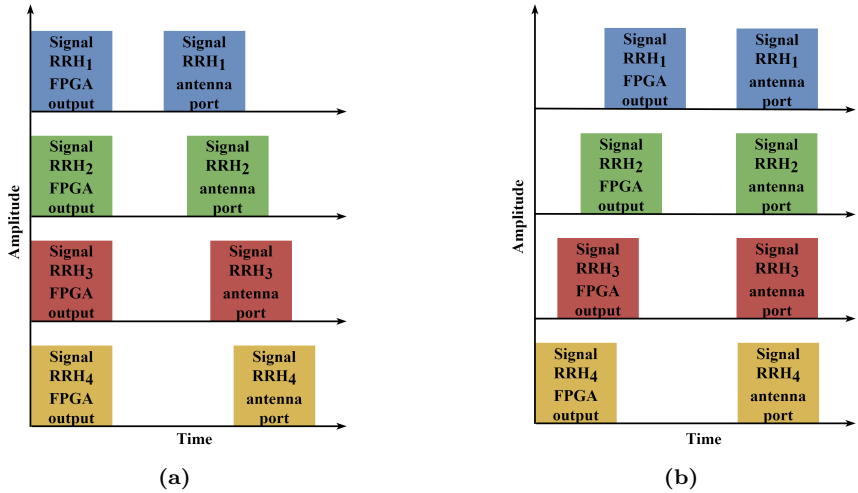

Figure 4.5: Visualization of the time delay effect. In (a) the signals to the remote radio heads (RRHs) are time-synchronized at the FPGA output, resulting in that they are un-synchronized at the antenna port outputs. In (b) the signals are time-synchronized at the antenna port output, by delaying them in the central-unit so they are un-synchronized at the FPGA output.

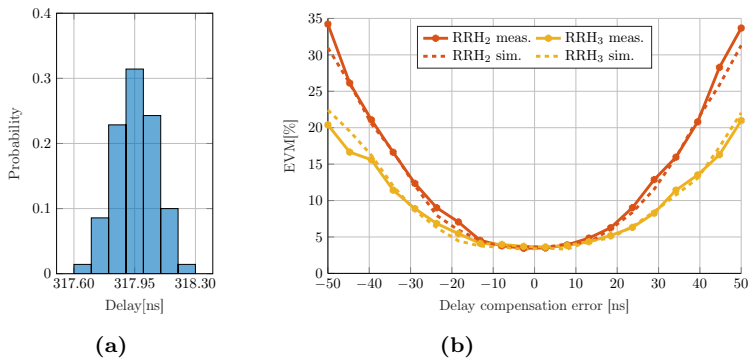

Figure 4.6: (a) Histogram of 70 consecutive measurements of time delay difference between remote radio head (RRH) 3 and RRH_4. (b) Measurements and simulations of EVM versus delay compensation error for RRH_2 and RRH_3, on at a time. Delay compensation error refers to time offset compared to the ideal delay compensation [Paper C].

In Fig. 4.5a a visualization of the signal to each RRH when not applying time delay compensation is shown. The signals are then time-synchronized at the output of the FPGA, but due to the fiber length differences they are not when arriving at the RRH antenna port. However, when applying time delay compensation as in Fig. 4.5b the signals are no longer time-synchronized at the FPGA output, but at the antenna port.

We evaluated the method using a measurement setup with four serially connected RRHs, and 60 m fiber in between each. In Fig. 4.6a the histogram of 70 consecutive measurements of the time-delay difference between two serially connected RRHs is shown. The measured delay varies less than 1 ns and is uniformly centered around the average value. The method provides sufficient

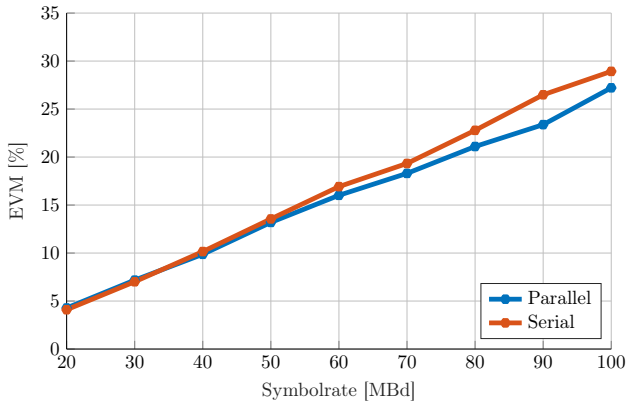

Figure 4.7: Measured error vector magnitude (EVM) for the proposed architecture with four serial and parallel connected RRHs [Paper C]. For the serially connected remote radio heads (RRHs) time-delay compensation is applied.

accuracy, as introducing a delay compensation error of 1 ns from the correct gives insignificant effect on EVM. This is shown in Fig. 4.6b where EVM is presented versus delay compensation error.

For the benefit in scalability to be valuable, a system with serially connected RRHs has to perform equally good as one with RRHs connected in parallel. In Fig. 4.7 the measured EVM is presented versus symbolrate, showing that serial connection of RRHs does not degrade the EVM performance significantly compared to parallel connected RRHs, as long as the previously described time delay compensation method is applied.

4.4.2 Power Constraints

The maximum number of RRHs that can be connected in series is limited by the minimium required input power to the OT in the RRH furthest away from the CU. The OTs used in the proposed architecture require a minimum optical input power of −15 dBm. The optical input power to the furthest OT is decided by: the optical output power from the transmitting OT at the CU, the total fiber length and the number of OADMs passed. The received power at the furthest RRH in dBm is

$$P_{rx,N,dBm} = P_{tx,dBm} - \alpha_f LN - \alpha_p(N-1), \tag{4.2}$$

where $P_{tx,dBm}$ is the output power of the transmitting OT in dBm, α_f is the fiber loss in dB/meter, L is the fiber length between each RRH in meter, N is the total number of RRHs and α_p is the average OADM pass loss in dB.

In Fig. 4.8 the optical input power to the furthest RRH versus total number of RRHs is presented. $\alpha_f = 0.22$ dB/km has been extracted from the datasheet, $\alpha_p = 0.3$ dB and $P_{tx} = 2$ dBm have been measured in the setup. For the configuration presented in [Paper C], with a fixed fiber length of 60 m between each RRH, Fig. 4.8 shows that 55 RRHs could be serially connected before the power to the furthest RRH is too low. Although, limiting the number of RRHs to the 18 standardized CWDM wavelengths [51], the fiber length could be extended up to 3 km optical fiber between each RRHs.

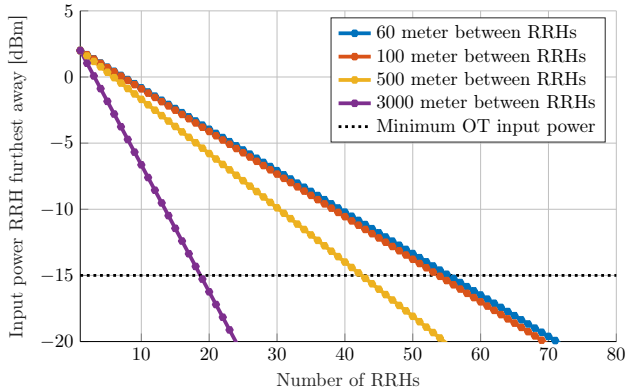

Figure 4.8: Input optical power to the remote radio head (RRH) furthest away from the central-unit (CU) versus number of RRHs, for 60 and 3000 m fiber length between each RRH. Also the minimum optical transceiver (OT) power of −15 dBm is presented, which limits the number of RRHs.

4.5 Multi-User MIMO Measurements

As a final demonstration of the architecture proposed in Fig. 4.2, this section presents MU-MIMO measurements. Four RRHs connected in series serve two users simultaneously, using the same time- and frequency resources and spatial multiplexing. ZF-precoding is applied, which minimizes inter-user interference.

Fig. 4.9 shows the constellation diagrams of the received demodulated symbols, with a measured EVM of 10.4 % for UE_1 and 6.2 % for UE_2. Some distortion is shown in the constellation diagrams; to evaluate it the error spectrum is presented in Fig. 4.9c for UE_1 and Fig. 4.9d for UE_2. The error spectrum is the difference between the transmitted and received constellation symbols, presented in frequency domain. The error indicates that some interference still occurs as the power level within the signal bandwidth is higher than the noise floor. Different explanations for this could be: non-ideal channel estimation resulting in sub-optimal ZF precoding, interference between channels in the FPGA or electromagnetic coupling between the RF circuit boards at the CU or RRHs. Further research is needed to isolate the source, but a certain level of leakage has been measured between the FPGA channels making it a viable candidate.

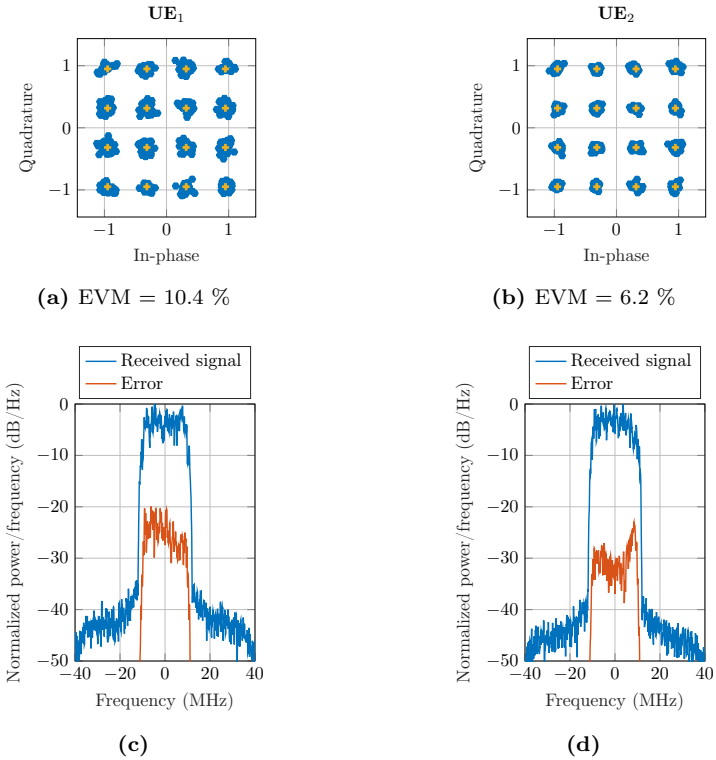

(a) EVM = 10.4 %

(b) EVM = 6.2 %

(c)

(d)

Figure 4.9: Constellation diagrams of the received symbols using zero-forcing (ZF) precoding for two user equipments (UEs), (a) UE_1, EVM= 10.4 % and (b) UE_2, EVM = 6.2 % The normalized power spectral density of the received signal after down-conversion to baseband as well as the error are presented for (c) UE_1 and (d) UE_2. The error is an up-sampled frequency domain representation of the difference between the transmitted and received symbols [Paper C].

4.6 Chapter Summary

This chapter reviewed previous work on ARoF and SDoF testbed architectures for D-MIMO. It was proposed that scalability of D-MIMO networks could be enhanced by connecting the RRHs in series instead of in parallel. Potential challenges that arise in a system with different fiber lengths to each RRH were discussed based on measurement results from [Paper B] and [Paper C]. For the problem with different time delay, two time delay compensation methods were presented. OTA measurements showed that serial connection of RRHs does not compromise system performance, compared to parallel connection of RRHs. Finally MU-MIMO measurements confirmed that by applying appropriate time delay compensation, the architecture with serial connected RRHs can be used for MU-MIMO.

Chapter 5

Conclusions and Future Work

5.1 Conclusions

The increasing demand on wireless connectivity puts high requirements on the mobile communication systems in terms of coverage, capacity, latency and reliability. New innovative approaches are needed to meet these requirements. At the same time all major infrastructure must to be energy efficient to not contribute negatively to climate change. D-MIMO is considered a promising technology to increase coverage, capacity, latency and reliability, while also being energy efficient.

In D-MIMO many distributed RRHs are used, in difference from a traditional mimo system which uses one centralized base station with many co-located antenna elements. The improved energy efficiency results from that a user is assumed to always be in the proximity of at least one RRH, so the transmit power is used more efficiently than with one centralized base station. However, how to implement D-MIMO is not trivial and depends highly on the level of synchronization needed among the RRHs for a specific deployment.

This thesis has described the background and motivation for using D-MIMO, and how the most gain is achieved when operating the RRHs phase synchronized. The challenges of implementing phase synchronized distributed RRHs have been addressed, with the proposed solution of doing central frequency up-conversion and transmitting RF-signals over the fronthaul.

Moreover it has been stated that implementing the fronthaul with direct RF-transmission makes RoF a good candidate, and different RoF technologies have been described and compared. SDoF was found to have certain advantages compared to ARoF in terms of robustness towards non-linearities and optical inter-channel interference. Moreover, the challenge of making a D-MIMO system scalable as the number of RRHs increase was addressed, by suggesting serial connection of the RRHs using WDM. Finally, a D-MIMO architecture with SDoF fronthaul and four serially connected RRHs was implemented. Measurement results showed that the proposed architecture can serve two users with the same time- and frequency resources, using spatial multiplexing.

In summary, this thesis has addressed the challenges of implementing D-MIMO, and investigated one potential solution using central frequency up-conversion, SDoF fronthaul and serially connected RRHs. The results in this thesis provide several insights into the realization of future communication systems.

5.2 Future Work

Based on the conclusions in this thesis and demand on future communication systems, we believe that the following topics are interesting directions for future research

- **Bandwidth limitations of SDM.** The level of quantization noise is highly dependent on the oversampling-ratio, but there is a limitation on how fast a realistic system can sample. As a consequence the symbolrate is limited. If SDM should be a competitive candidate new approaches to overcome this has to be investigated.
- **SDoF mm-wave solutions.** mm-wave solutions for SDoF have been investigated, but more work is needed. One interesting direction is to explore optical up-conversion, that is commonly used in ARoF links.
- **Serial connection with uplink.** It is necessary to investigate what challenges that arise when extending the architecture with WDM serial connection of the RRHs to also include uplink. The OTs, MUXs and OADMs are dual fiber components, hence the WDM serial connection presented in this thesis can be combined with the 1-bit uplink concept demonstrated in [25] to create a time-division duplex D-MIMO testbed with serially connected RRHs.

Acknowledgements

I would like to thank all the people who have supported me in my PhD work so far: friends, family and all colleagues at MEL and TML.

A big thank you to my main supervisor Prof. Christian Fager for first of all awakening my interest in wireless communication systems in the first course during the master program. Without your pedagogical lectures and great commitment to teaching us students back then, I do not think I would have developed such an interest in this field. But also thanks for supporting me now throughput the PhD, always being available and encouraging when I bring up new ideas, while simultaneously giving enough resistance so that I move forward!

I would also like to thank my examiner Prof. Magnus Karlsson and co-supervisor Prof. Thomas Eriksson. You are always available when I have questions, and even though it can be challenging doing multi-disciplinary research you always show an interest in finding the common grounds and bringing us into new interesting discussions and research directions.

A huge thank to my friend and co-PhD student Lise Aabel! I do not think I would have come this far in my research if it was not for you, and our cooperation. Having someone that works with something really close to your own PhD topic that is also your friend is invaluable, as new ideas come up both in the coffee break at work and the weekend dinners, thank for that again!

Last but not least, I would like to express my immense gratitude to my family and all my friends. First of all, my parents, who have always told me that I can do whatever I want, making me unafraid to try new things. I also want to extend enormous gratitude to my partner Jonathan, for supporting me and taking extra shifts in juggling family life when I have to put in extra effort at work. A supportive partner is what makes it possible to pursue a PhD when you have small kids. Finally, thanks to my son Ruben for being the best distraction from a stressful day. It is invaluable!

This work was financed by the Swedish Research Council through grant VR-2019-05174

Bibliography

[1] Ericsson, "Ericsson mobility report," Ericsson, Tech. Rep., 2024, accessed: 2024-06-13. [Online]. Available: https://www.ericsson.com/en/reports-and-papers/mobility-report/reports/business-review

[2] U. C. Bureau, "U.s. and world population clock," 2024. [Online]. Available: https://www.census.gov/popclock/world

[3] M. A. Uusitalo, P. Rugeland, M. R. Boldi, E. C. Strinati, P. Demestichas, M. Ericson, G. P. Fettweis, M. C. Filippou, A. Gati, M. H. Hamon, M. Hoffmann, M. Latva-Aho, A. Parssinen, B. Richerzhagen, H. Schotten, T. Svensson, G. Wikstrom, H. Wymeersch, V. Ziegler, and Y. Zou, "6G Vision, Value, Use Cases and Technologies from European 6G Flagship Project Hexa-X," *IEEE Access*, vol. 9, pp. 160 004–160 020, Nov. 2021.

[4] G. Wikström, P. Persson, S. Parkvall, G. Mildh, E. Dahlman, B. Balakrishnan, P. Öhlén, E. Trojer, G. Rune, J. Arkko, Z. Turányi, D. Roeland, B. Sahlin, W. John, J. Halén, and H. Björkegren, "6G – Connecting a cyber-physical world," Ericsson, Stockholm, Sweden, Ericsson white paper, 2022.

[5] S. Zhou, M. Zhao, X. Xu, J. Wang, and Y. Yao, "Distributed wireless communication system: A new architecture for future public wireless access," *IEEE Commun. Mag.*, vol. 41, no. 3, pp. 108–113, Mar. 2003.

[6] A. Goldsmith, *Wireless Communications*. Cambridge, United Kingdom: Cambridge Univ. Press, 2005.

[7] G. Corazza, "Marconi's history [radiocommunication]," *Proc. of the IEEE*, vol. 86, no. 7, pp. 1307–1311, Jul. 1998.

[8] T. Mshvidobadze, "Evolution mobile wireless communication and LTE networks," in *2012 6th Int. Conf. on Application of Inf. and Commun. Technol.*, Oct. 2012, pp. 1–7.

[9] L. M. Larsen, A. Checko, and H. L. Christiansen, "A survey of the functional splits proposed for 5G mobile crosshaul networks," *IEEE Commun.s Surv. and Tut.*, vol. 21, no. 1, pp. 146–172, Oct. 2019.

[10] G. J. Foschini, "Layered space-time architecture for wireless communication in a fading environment when using multi-element antennas," *Bell Labs Tech. J.*, vol. 1, no. 2, pp. 41–59, 1996.

[11] J. Vieira, F. Rusek, O. Edfors, S. Malkowsky, L. Liu, and F. Tufvesson, "Reciprocity calibration for massive MIMO: Proposal, modeling, and validation," *IEEE Trans. on Wireless Commun.*, vol. 16, no. 5, pp. 3042–3056, May 2017.

[12] T. Lo, "Maximum ratio transmission," *IEEE Trans. on Commun.*, vol. 47, no. 10, pp. 1458–1461, Oct. 1999.

[13] I. C. Sezgin, M. Dahlgren, T. Eriksson, M. Coldrey, C. Larsson, J. Gustavsson, and C. Fager, "A low-complexity distributed-MIMO testbed based on high-speed sigma–delta-over-fiber," *IEEE Trans. Microw. Theory Technol.*, vol. 67, no. 7, pp. 2861–2872, Mar. 2019.

[14] H. Bao, I. C. Sezgin, Z. S. He, T. Eriksson, and C. Fager, "Automatic Distributed MIMO Testbed for beyond 5G Communication Experiments," in *IEEE MTT-S Int. Microw. Symp. Digest.* IEEE, Jun. 2021, pp. 697–700.

[15] C. Fager, S. Rimborg, E. Radahl, H. Bao, and T. Eriksson, "Comparison of Co-located and Distributed MIMO for Indoor Wireless Communication," in *IEEE Radio and Wireless Symp., RWS*, Jan. 2022, pp. 83–85.

[16] H. Q. Ngo, A. Ashikhmin, H. Yang, E. G. Larsson, and T. L. Marzetta, "'Cell-Free Massive MIMO Versus Small Cells'," *IEEE Transactions on Wireless Communications*, vol. 19, no. 5, pp. 3623–3624, 2020.

[17] Ö. T. Demir, E. Björnson, and L. Sanguinetti, *Foundations of User-Centric Cell-Free Massive MIMO*, Boston, MA, USA, 2021.

[18] E. Björnson and L. Sanguinetti, "Making cell-free massive MIMO competitive with mmse processing and centralized implementation," *IEEE Trans. on Wireless Commun.*, vol. 19, no. 1, pp. 77–90, Sep. 2020.

[19] E. G. Larsson, "Massive Synchrony in Distributed Antenna Systems," *IEEE Trans. on Signal Process.*, vol. 72, pp. 855–866, Jan. 2024.

[20] H. Bao, F. Ponzini, and C. Fager, "Wideband mm-wave 6 × 2 distributed MIMO transmitter using sigma-delta-over-fiber," *J. of Lightw. Technol.*, vol. 42, no. 9, pp. 3107–3117, Jan. 2024.

[21] C. Y. Wu, H. Li, O. Caytan, J. Van Kerrebrouck, L. Breyne, J. Bauwelinck, P. Demeester, and G. Torfs, "Distributed Multi-User MIMO Transmission Using Real-Time Sigma-Delta-Over-Fiber for Next Generation Fronthaul Interface," *J. of Lightw. Technol.*, vol. 38, no. 4, pp. 705–713, Oct. 2020.

[22] O. Simeone, U. Spagnolini, Y. Bar-Ness, and S. H. Strogatz, "Distributed synchronization in wireless networks," *IEEE Signal Process. Mag.*, vol. 25, no. 5, pp. 81–97, Sep. 2008.

[23] C. Y. Wu, H. Li, O. Caytan, J. Van Kerrebrouck, L. Breyne, J. Bauwelinck, P. Demeester, and G. Torfs, "Distributed Multi-User MIMO Transmission Using Real-Time Sigma-Delta-Over-Fiber for Next Generation Fronthaul Interface," *J. of Lightw. Technol.*, vol. 38, no. 4, pp. 705–713, Oct. 2020.

[24] R. Puerta, M. Joharifar, M. Han, A. Djupsjöbacka, V. Bobrovs, S. Popov, O. Ozolins, and X. Pang, "Experimental Validation of Coherent Joint Transmission in a Distributed-MIMO System with Analog Fronthaul for 6G," in *2023 Joint European Conf. on Netw. and Commun. and 6G Summit*, Jun. 2023, pp. 585–590.

[25] L. Aabel, S. Jacobsson, M. Coldrey, F. Olofsson, G. Durisi, and C. Fager, "A TDD distributed MIMO testbed using a 1-bit radio-over-fiber fronthaul architecture," *IEEE Trans. Microw. Theory Technol.*, Apr. 2024, early Access.

[26] Ericsson, Huawei, Nec, and Nokia, "Common public radio interface," 2019. [Online]. Available: https://www.itu.int/rec/T-REC-G.694.2/en

[27] C. Lim and A. Nirmalathas, "Radio-Over-Fiber Technology: Present and Future," *J. of Lightw. Technol.*, vol. 39, no. 4, pp. 881–888, Feb. 2021.

[28] L. Zhang, D. Liu, W. Tong, S. Popov, G. Jacobsen, W. Hu, S. Xiao, J. Chen, A. Udalcovs, R. Lin, O. Ozolins, X. Pang, L. Gan, R. Schatz, M. Tang, and S. Fu, "Toward terabit digital radio over fiber systems: Architecture and key technologies." *IEEE Commun. Mag.*, vol. 57, no. 4, pp. 131 – 137, Mar. 2019.

[29] M. Hunukumbure, S. Electronics, L. D. Cea-leti, M. Castañeda, and H. Technologies, "to Provide an Immersive Experience to the Early 5G Adopters," in *ETSI Workshop on Future Radio Technol. - Air Interfaces*, Jan. 2016, pp. 1–10.

[30] R. Vaughan, N. Scott, and D. White, "The theory of bandpass sampling," *IEEE Trans. on Signal Process.*, vol. 39, no. 9, pp. 1973–1984, Sep. 1991.

[31] P. A. Gamage, A. Nirmalathas, C. Lim, D. Novak, and R. Waterhouse, "Design and analysis of digitized RF-over-fiber links," *J. of Lightw. Technol.*, vol. 27, no. 12, pp. 2052–2061, Jun. 2009.

[32] J.-M. Liu, *Photonic devices.* Cambridge, United Kingdom: Cambridge Univ. Press, 2005.

[33] Y. Li, Q. Xie, M. El-Hajjar, and L. Hanzo, "Analogue radio over fiber for next-generation ran: Challenges and opportunities," arXiv preprint arXiv:2111.13851, 2021, online [Accessed on: 2024-07-11]. [Online]. Available: https://arxiv.org/abs/2111.13851

[34] R. Heidemann, "Optical generation of very narrow linewidth millimetre wave signals," *Electron. Lett.*, vol. 28, no. 25, pp. 3–5, Dec. 1992.

[35] Y. Tian, K. L. Lee, C. Lim, and A. Nirmalathas, "Performance evaluation of comp for downlink 60-ghz radio-over-fiber fronthaul," in *2017 Int. Topical Meeting on Microw. Photon.*, dec 2017, pp. 1–4.

[36] L. Breyne, G. Torfs, X. Yin, P. Demeester, and J. Bauwelinck, "Comparison Between Analog Radio-Over-Fiber and Sigma Delta Modulated Radio-Over-Fiber," *IEEE Photon. Technol. Lett.*, vol. 29, no. 21, pp. 1808–1811, Sep. 2017.

[37] S. Pavan, R. Schreier, and G. C. Temes, *Understanding Delta-Sigma Data Converters*, 2nd ed. Hoboken, NJ, USA: John Wiley & Sons, 2017.

[38] L. M. Pessoa, J. S. Tavares, D. Coelho, and H. M. Salgado, "Experimental evaluation of a digitized fiber-wireless system employing sigma delta modulation," *Opt. Express*, vol. 22, no. 14, p. 17508, Jul. 2014.

[39] E. Hamed, H. Rahul, M. A. Abdelghany, and D. Katabi, "Real-time distributed MIMO systems," in *Proc. of the 2016 ACM Conf. on Special Interest Group on Data Commun.*, Aug. 2016, pp. 412–425.

[40] V. Yenamandra and K. Srinivasan, "Vidyut: Exploiting Power Line Infrastructure For Enterprise Wireless Networks," *ACM SIGCOMM Comput. Commun. Rev.*, vol. 44, no. 4, pp. 595–606, Aug. 2015.

[41] H. V. Balan, R. Rogalin, A. Michaloliakos, K. Psounis, and G. Caire, "AirSync: Enabling distributed multiuser MIMO with full spatial multiplexing," *IEEE/ACM Trans. on Netw.*, vol. 21, no. 6, pp. 1681–1695, Jan. 2013.

[42] D. Loschenbrand, M. Hofer, L. Bernado, S. Zelenbaba, and T. Zemen, "Towards Cell-Free Massive MIMO: A Measurement-Based Analysis," *IEEE Access*, vol. 10, pp. 89 232–89 247, Aug. 2022.

[43] C. Ranaweera, E. Wong, A. Nirmalathas, C. Jayasundara, and C. Lim, "5G C-RAN with optical fronthaul: An analysis from a deployment perspective," *J. of Lightw. Technol.*, vol. 36, no. 11, pp. 2059–2068, Jun. 2018.

[44] A. Moerman, J. Van Kerrebrouck, O. Caytan, I. L. De Paula, L. Bogaert, G. Torfs, P. Demeester, M. Moeneclaey, H. Rogier, and S. Lemey, "mmWave-over-Fiber Distributed Antenna Systems for Reliable multi-Gbps Wireless Communication," in *2022 3rd URSI Atlantic and Asia Pacific Radio Sci. Meeting*, Jun. 2022, pp. 1–4.

[45] L. Cheng, M. M. U. Gul, F. Lu, M. Zhu, J. Wang, M. Xu, X. Ma, and G. K. Chang, "Coordinated Multipoint Transmissions in Millimeter-Wave Radio-Over-Fiber Systems," *J. of Lightw. Technol.*, vol. 34, no. 2, pp. 653–660, Jan. 2016.

[46] M. Sung, J. H. Lee, J. Kim, E. S. Kim, S. H. Cho, Y. J. Won, B. C. Lim, S. Y. Pyun, H. Lee, and J. K. Lee, "RoF-Based Radio Access Network for 5G Mobile Communication Systems in 28 GHz Millimeter-Wave," *J. of Lightw. Technol.*, vol. 38, no. 2, pp. 409–420, Jan. 2020.

[47] R. F. Cordeiro, A. S. R. Oliveira, and J. Vieira, "All-digital transmitter with rof remote radio head," in *2014 IEEE MTT-S International Microwave Symposium*, Jun. 2014, pp. 1–4.

[48] H. Li, M. Verplaetse, J. Verbist, J. Kerrebrouck Van, L. Breyne, C.-Y. Wu, L. Bogaert, B. Moeneclaey, X. Yin, J. Bauwelinck, P. Demeester, and G. Torfs, "Real-Time 100-GS/s Sigma-Delta Modulator for All-Digital Radio-Over-Fiber Transmission," *J. of Lightw. Technol.*, vol. 38, no. 2, pp. 386–393, Jan. 2020.

[49] G. Interdonato, E. Björnson, H. Quoc Ngo, P. Frenger, and E. G. Larsson, "Ubiquitous cell-free Massive MIMO communications," *Eurasip J. on Wireless Commun.s and Netw.*, vol. 197, no. 1, pp. 1–13, Aug. 2019.

[50] Ericsson, "Radio stripes: re-thinking mobile networks," Ericsson, Stockholm, Sweden, 2019. [Online]. Available: https://www.ericsson.com/en/blog/2019/2/radio-stripes

[51] ITU, "G.694.2 : Spectral grids for WDM applications: Cwdm wavelength grid," 2019. [Online]. Available: https://www.itu.int/rec/T-REC-G.694.2/en

[52] A. Borsali, H. Badaoui, M. Aichi, and W. Aichi, "Effect of channel wavelength spacing for wdm system on the quality of the transmission," *Int. J. of Computer Sci. Issues*, vol. 9, May 2012.

[53] K. Ito, M. Suga, Y. Shirato, N. Kita, and T. Onizawa, "Remote Beamforming Scheme with Fixed Wavelength Allocation for Radio-Over-Fiber Systems Employing Single-Mode Fiber," *J. of Lightw. Technol.*, vol. 40, no. 4, pp. 997 – 1006, Feb. 2021.

[54] M. B. Othman, L. Deng, X. Pang, J. Caminos, W. Kozuch, K. Prince, J. Bevensee Jensen, and I. Tafur Monroy, "Directly-modulated VCSELs for 2x2 MIMO-OFDM radio over fiber in WDM-PON," in *2011 37th European Conference and Exhibition on Optical Communication*, Sep. 2011, pp. 1–3.

[55] E. Ruggeri, A. Tsakyridis, C. Vagionas, G. Kalfas, R. M. Oldenbeuving, P. W. L. van Dijk, C. G. Roeloffzen, Y. Leiba, N. Pleros, and A. Miliou, "A 5G fiber wireless 4Gb/s WDM fronthaul for flexible 360° coverage in V-band massive MIMO small cells," *J. of Lightw. Technol.*, vol. 39, no. 4, pp. 1081–1088, Oct. 2021.

[56] E.-S. Kim, M. Sung, J. H. Lee, J. K. Lee, S.-H. Cho, and J. Kim, "Coverage extension of indoor 5G network using rof-based distributed antenna system," *IEEE Access*, vol. 8, pp. 194 992–194 999, Oct. 2020.

[57] K. Tsukamoto, T. Nishiumi, T. Yamagami, T. Higashino, S. Komaki, R. Kubo, T. Taniguchi, J. I. Kani, N. Yoshimoto, H. Kimura, and K. Iwatsuki, "Convergence of WDM access and ubiquitous antenna architecture for broadband wireless services," *Piers Online*, vol. 1, pp. 773–777, Jan. 2010.

[58] R. W. Chang, "Synthesis of Band-Limited Orthogonal Signals for Multichannel Data Transmission," *Bell System Tech. J.*, vol. 45, no. 10, pp. 1775–1796, Dec. 1966.

[59] S. B. Weinstein, "The history of orthogonal frequency-division multiplexing," *IEEE Commun. Mag.*, vol. 47, no. 11, pp. 26–35, Nov. 2009.

[60] Y. Fan, A. E. Aighobahi, N. J. Gomes, K. Xu, and J. Li, "Performance analysis of commercial multiple-input-multiple-output access point in distributed antenna system," *Opt. Express*, vol. 23, no. 6, pp. 7500–7513, Mar 2015.